Measurement of Instability Growth in a Magnetized *Z* Pinch in the Finite-Larmor-Radius Regime

H. M. Davies, A. E. Dangor, M. Coppins, and M. G. Haines
The Blackett Laboratory, Prince Consort Road, London SW7 2BZ United Kingdom
(Received 11 April 2001; published 18 September 2001)

The development of the $m = 0$ instability in a Z pinch was followed and the measured growth rates compared with 2D MHD simulations. Where MHD is valid, the measured growth rates agree well with simulation. Where the ions are magnetized, i.e., where the ion-cyclotron frequency is smaller than the ion-collision frequency and the ratio of the ion Larmor radius to pinch radius is of the order of 0.1, the growth rate was smaller than expected by a factor of 2.5. This is as predicted by finite-Larmor-radius theory. The product of the wave number and the pinch radius was $ka \sim 2\pi$ and was the same for all conditions. Perturbations as large as 30% of the pinch radius were observed; no nonlinear saturation was evident.

DOI: 10.1103/PhysRevLett.87.145004 PACS numbers: 52.58.Lq

The linear Z pinch, in which plasma is confined by the interaction of the axial current with its self-generated azimuthal magnetic field, has been studied extensively. From the earliest experiments [1], the Z pinch was found to be unstable, particularly to the $m = 0$ (sausage) instability. Analysis based on ideal MHD [2] shows that the Z pinch is always $m = 1$ (kink) unstable and that $m = 0$ is stable only if the pinch current is strongly peaked on axis and the pressure at the edge is finite. This has been experimentally verified in a gas-embedded pinch [3].

Ideal MHD is valid only if (i) ions are collisional, i.e., the ratio of the ion-collision time to the radial Alfvén transit time is small ($\tau_{ii} a/v_A \ll 1$); (ii) ion Larmor radius is negligible, i.e., the ratio of the average Larmor radius to the pinch radius is small ($\varepsilon = a_i/a \ll 1$); and (iii) resistivity η is low, i.e., the magnetic Reynolds number is large ($R_m = \mu_0 v_A a/\eta \gg 1$). These conditions are valid only for a very limited range of parameters [4]. When the ion Larmor radius is finite and the ions are magnetized (i.e., $a_i/a > 0.1$, $\Omega_{ci}\tau_{ii} > 1$) the pinch is in the finite-Larmor-radius (FLR) regime (here $R_m \gg 1$). FLR effects are known theoretically to stabilize the rotating θ pinch [5]. However, the strong magnetic field curvature and field null on axis prevent extension of analytical FLR theory to the Z pinch. Analysis based on the Vlasov model [6] (in which the ions are treated kinetically) has shown that absolute stability is never attained. A reduction of the growth rate for small perturbations is predicted, by a factor of up to 3 for $m = 0$ and 10 for $m = 1$, the maximum reduction being in the range $0.1 < a_i/a < 0.2$, for $ka = 6$. Using a hybrid code, Arber [7] found no saturation at large amplitudes in an FLR pinch, the growth rate being reduced by a factor of 1.8 [8]. In this paper, we present the first experimental evidence of FLR effects in a Z pinch where the ions are magnetized.

The Z pinch was driven by a current pulse (160 kA peak, 65 ns 10%–90% rise time, 30 ns plateau, and 100 ns fall) produced by a pulsed-power generator. The pinch was formed within a 20 mm internal diameter quartz tube between electrodes 60 mm apart, static filled with hydrogen from 1 to 3 mbar. The pinch was diagnosed with optical streak and four-frame gated image intensifier cameras. The collapse dynamics are compared with a 1D Lagrangian, two-fluid, resistive, MHD code [9]. A 2D Eulerian MHD

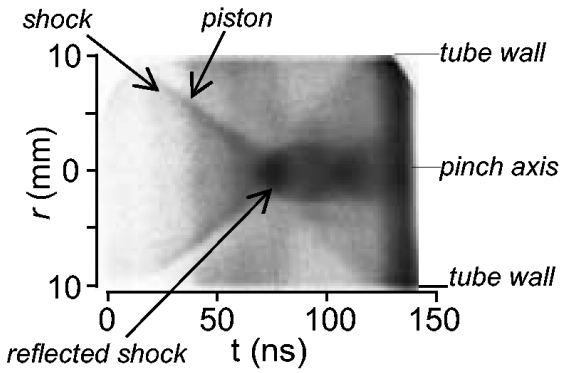

FIG. 1. Side-on radial streak photograph at 3 mbar. Time zero is at the start of the current. Image is corrected for tube distortion.

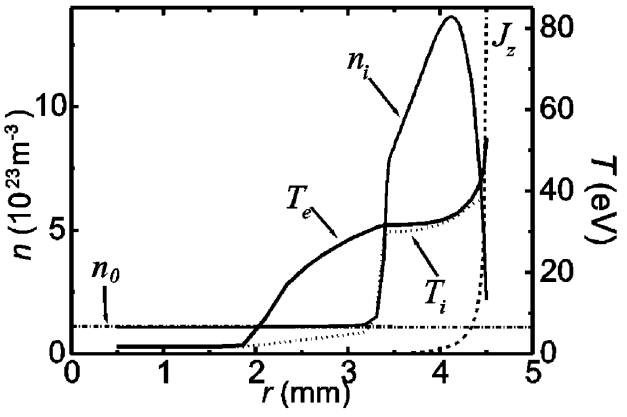

FIG. 2. Pinch profiles from 1D MHD simulation at 70 ns. Initial fill density n_0 corresponds to 3 mbar. J_z is in arbitrary units.

 0031-9007/01/87(14)/145004(4)$15.00

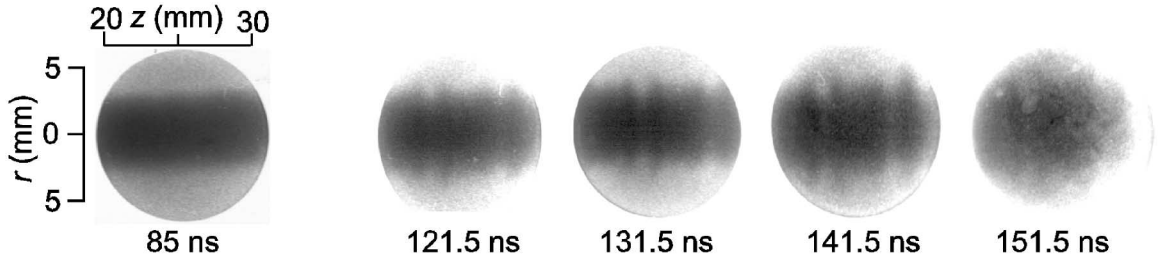

FIG. 3. Optical framing photographs at 3 mbar. First image is 10 ns after pinch formation. The remaining images are from the same shot.

code [10] is used to simulate the instability growth from equilibrium.

Streak photography showed that the current flowed initially at the wall and that the $\mathbf{J} \times \mathbf{B}$ force drove a magnetic piston towards the axis. A typical streak is shown in Fig. 1. Since the collapse was supersonic, a shock was generated ahead of the piston. The piston velocity was found to decrease slowly with pressure, as expected. The ratio of the shock and piston velocities was measured to be $v_s/v_p \approx 4/3$, which is the value for a strong shock in a monatomic gas ($\Gamma = 5/3$). The radial distributions of the current, ion and electron number densities and temperatures during the collapse from the 1D MHD simulation are shown in Fig. 2. The current is confined to a thin shell at the piston and this gives rise to the large electron temperature peak. The shock and piston velocities are lower than observed but the ratio v_s/v_p is still close to $4/3$. The density jump across the shock is about 8. Within the shocked plasma, the electrons and ions are at the same temperature. Strong electron thermal conduction produces the electron temperature pedestal ahead of the shock. The ions are not preheated here, because ion thermal conduction is small and the time for electron-ion energy transfer in this region is long. The integrated bremsstrahlung emission, calculated from the temperature and density distributions in the simulation, compares reasonably well with line outs of the streak film exposure.

The streak image (Fig. 1) shows that, on reaching the axis, the shock was reflected. At this time there was a dramatic increase in radiation from the plasma. The pinch was formed when the reflected shock reached the incoming piston. Thereafter, the pinch radius changed only slightly. The first frame in Fig. 3 (taken 10 ns after pinch formation) shows a well-defined stable plasma column. The radius of the pinch column varied weakly with fill pressure. The low intensity front expanding from the pinch in Fig. 1 is presumed to be an artifact, since it was not seen in framing photographs and the apparent velocity of this front was independent of pressure. There was no rapid, gross expansion of the plasma column after pinch formation, as should occur when the current decreases. This is due to a crowbar of the pinch current through a plasma formed at the wall by radiation from the pinch. The current in the pinch was thus isolated from the external circuit and the magnetic flux between the pinch and the wall trapped, preventing any significant expansion of the pinch. The decay time of the crowbarred current is calculated to be a few hundred nanoseconds from the inductance and resistance of the current path (assuming the wall plasma temperature $\sim$10 eV and thickness $\sim$1 mm). The 1D MHD code is able to simulate the observed radial dynamics only if the current crowbar is assumed, i.e., the current waveform is taken to be the measured current up to the time of pinch formation, and thereafter kept constant. Without the crowbar, the code predicts a very rapid expansion to the wall. With the crowbar, there is a radial oscillation of the column, which remained within the measured pinch radius. It should be noted that the ion mean free path becomes comparable with the shell width near the end of the collapse. This is not consistent with the assumption that the ions are collisional in MHD and may account for the rapid oscillation which is not seen in the experiment.

Table I lists the pinch parameters at different pressures. Also tabulated are two estimates of pinch temperature, T_B, obtained from the Bennett relation $8\pi(1 + Z_{\text{eff}})Nk_BT_B = \mu_0 I^2$, and T_c, estimated from the final measured piston velocity v_{final} using $(3/2)(1 + Z_{\text{eff}})k_BT_c = (1/2)(1 + A_{\text{eff}})m_p v_{\text{final}}^2$, which assumes that the kinetic energy is

TABLE I. Pinch parameters and the temperatures T_B from the Bennett relation, T_c from the collapse dynamics.

p_0 (mbar)	N (10^{19} m^{-1})	I (kA)	a (mm)	v_{final} (10^{17} cm s^{-1})	T_B (eV)	T_c (eV)
1	1.61	155	2.2	2.8	220	273
1.5	2.53	162	2.2	1.9	158	126
2	3.38	160	2.5	1.6	118	89
3	5.07	156	2.5	1.2	69	50

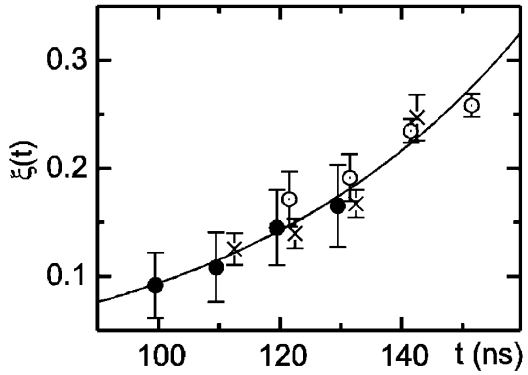

FIG. 4. Normalized amplitude $\xi(t)$ for the $m = 0$ instability for three shots at early (●), middle (×), and late (○) times at 3 mbar. The error bars represent variation in amplitudes in a single frame. The line is the best fit exponential to all the points. The average ka was measured to be 7.0 ± 0.4.

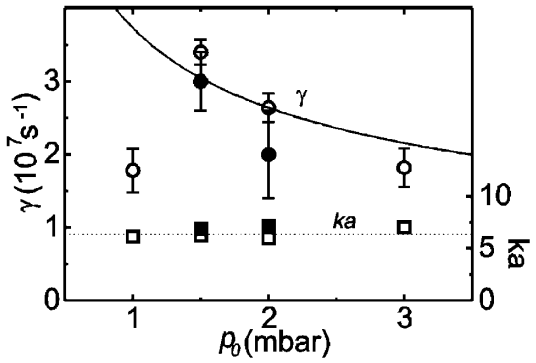

FIG. 5. The growth rate and ka versus fill pressure for experimental (●) and 2D MHD simulation (○). The curve is the predicted MHD scaling (proportional to $p_0^{1/2}$) normalized to the experimental point at 2 mbar.

thermalized. The error in T_B is estimated to be ~20% and that in T_c ~ 30%. These errors are comparable with the difference between T_B and T_c. Z_{eff} and A_{eff} are assumed to be 1. If an impurity was present, T_c and T_B would differ by far more.

Perturbations are not observed at the time of pinch formation and for some time thereafter (Fig. 3). Periodic, $m = 0$ perturbations are detected later, 30–40 ns after pinch formation. (The minimum detectable perturbation was about 5% of the column radius.) The sequence of four framing photographs in Fig. 3 shows typical instability structure in which $m = 0$ modes are dominant. The time evolution of individual bulges and necks was followed through the four frames and a normalized perturbation amplitude $\xi(t) = \delta a(t)/a$ calculated [$\delta a(t)$ is the measured displacement and a is the average measured pinch radius, approximately constant]. The averaged $\xi(t)$ is plotted in Fig. 4 for three shots at 3 mbar. The timing of the frames in the shots was changed, so that the instability was followed over a long time. The exponential growth rate, obtained by a best fit exponential to the data, is $\gamma = 2.1(\pm 0.2) \times 10^7\ \text{s}^{-1}$. The wavelength of the instability did not vary significantly with time, the average being $ka = 7.0 \pm 0.4$. The average growth rate and ka are plotted as a function of pressure in Fig. 5. For a pinch in Bennett equilibrium the growth rate scales as $N^{-1/2}$ [4], i.e., as $p_0^{-1/2}$. This scaling is included in the figure (solid line). The growth rate at 1 mbar does not vary with ideal MHD scaling, being a factor of ~2 lower.

Growth rates were also obtained from the 2D MHD simulation. The simulation followed the evolution of random density fluctuations imposed on a plasma column initially in a self-similar profile [11] with current and line density similar to the experiment. Transverse images, similar to what is shown in Fig. 6, were generated from the simulation by integrating the bremsstrahlung emission. These synthetic images were analyzed by the same method used for the experiment. The perturbations were plotted as a function of time and the average ka determined. The growth was found to be exponential and the growth rate obtained by a best fit. These growth rates and ka are plotted in Fig. 5. The experiment and simulation points agree well. As for the experiment, nonlinear saturation was not observed in the simulation (perturbations up to 45% were followed in the simulation).

In Table II we list values of a_i/a, $\Omega_{ci}\tau_{ii}$, and v_{thi}/a calculated at the temperature T_{av}, the average of T_B and T_c in Table I. ($v_{\text{thi}}/a = 3k_B T_{\text{av}}/m_i$ is the ion thermal velocity, a is from experiment.) Clearly, at 1 mbar the ions are magnetized. Also tabulated are the growth rates and ka's from experiment. The ratio $\gamma_{\text{expt}}/(v_{\text{thi}}/a)$ is the normalized growth rate. The normalized growth rate is the same for all pressures except in the magnetized case at 1 mbar, where it is a factor of 2.5 smaller. This is to be compared with results from the hybrid code [7,8], which found that the growth rate was reduced by a factor of 1.8 from the zero ion Larmor radius case. It should be noted that in the nonmagnetized regime the growth rate is closer to that calculated for the Vlasov fluid model in a skin current pinch than for the ideal MHD model [12]. The estimated magnetic field diffusion time is long compared to the growth time.

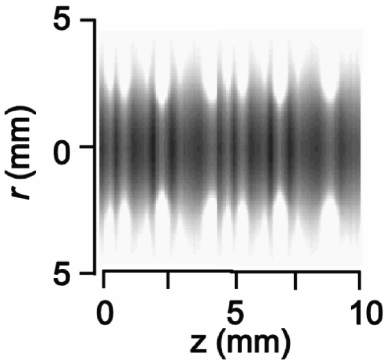

FIG. 6. Synthetic image from the 2D MHD code, for 2 mbar fill pressure.

TABLE II. Plasma parameters for average temperature T_{av}, average of T_B and T_c in Table I. $\gamma_{\mathrm{expt}}/(v_{\mathrm{thi}}/a)$ is the normalized growth rate, v_{thi} is the ion thermal velocity. γ_{expt} and ka_{expt} are from experiment.

p_0 (mbar)	a_i/a	$\Omega_{ci}\tau_{ii}$	v_{thi}/a (10^7 s^{-1})	γ_{expt} (10^7 s^{-1})	$\gamma_{\mathrm{expt}}/(v_{\mathrm{thi}}/a)$	ka_{expt}
1	0.15 ± 0.03	3.70 ± 1.1	8.7 ± 0.7	1.8 ± 0.3	0.21 ± 0.04	6.1 ± 0.1
1.5	0.11 ± 0.02	1.1 ± 0.3	6.6 ± 0.6	3.4 ± 0.2	0.52 ± 0.05	6.2 ± 0.2
2	0.09 ± 0.02	0.6 ± 0.2	5.0 ± 0.5	2.7 ± 0.1	0.54 ± 0.06	6.0 ± 0.1
3	0.08 ± 0.02	0.19 ± 0.06	3.6 ± 0.5	1.8 ± 0.3	0.51 ± 0.09	7.0 ± 0.4

In summary, we present here the first quantitative measurements of the growth of the $m = 0$ instability in the equilibrium phase of a Z pinch. Where ideal MHD is valid, there is close agreement of the growth rate and wavelength with 2D simulation, the growth rate scaling with the Alfvén transit time as suggested by theory. For a magnetized plasma with $a_i/a = 0.15$ the growth rate is reduced by a factor of 2.5, which agrees well with hybrid simulations [7,8]. The growth was exponential in both the ideal MHD and magnetized regimes, where FLR applies. The wavelength was such that $ka \sim 2\pi$ in both regimes. No saturation due to nonlinear effects was evident in either the experiment or the simulation.

The authors wish to acknowledge Dr. J. Chittenden for his advice regarding the 1D and 2D MHD codes, and Dr. F. Beg for his invaluable advice regarding the generator.

[1] R. Carruthers and P. A. Davenport, Proc. Phys. Soc. London Sect. B **70**, 49 (1957).
[2] B. B. Kadomstev, in *Reviews of Plasma Physics,* edited by M. A. Leontovich (Consultants Bureau, New York, 1966), Vol. 2, p. 153.
[3] P. Choi *et al.,* Nucl. Fusion **28**, 1771 (1988).
[4] M. G. Haines and M. Coppins, Phys. Rev. Lett. **66**, 1462 (1991).
[5] E. Bowers and M. G. Haines, Phys. Fluids **14**, 165 (1971).
[6] P. G. F. Russell *et al.,* Phys. Plasmas **4**, 2322 (1997).
[7] T. D. Arber, Phys. Rev. Lett. **77**, 1766 (1996).
[8] S. W. Channon, Ph.D. thesis, University of London, 2000.
[9] J. P. Chittenden and M. G. Haines, J. Phys. D. **26**, 1048 (1993).
[10] J. P. Chittenden *et al.,* Plasma Phys. **4**, 4309 (1997).
[11] M. Coppins, J. P. Chittenden, and I. D. Culverwell, J. Phys. D **25**, 178 (1992).
[12] T. D. Arber and M. Coppins, Phys. Fluids B **1**, 2289 (1989).